Plasmonic gap mode nanocavities at telecommunication wavelengths

Pi-Ju Cheng[a,b], Chen-Ya Weng[b,c], Shu-Wei Chang[a,b], Tzy-Rong Lin[c,d], and Chung-Hao Tien[a]

[a]Department of Photonics, National Chiao Tung University, Hsinchu 30010, Taiwan
[b]Research Center for Applied Sciences, Academia Sinica, Nankang, Taipei 11529, Taiwan
[c]Institute of Optoelectronic Sciences, National Taiwan Ocean University, Keelung 20224, Taiwan
[d]Department of Mechanical and Mechatronic Engineering, National Taiwan Ocean University, Keelung 20224, Taiwan

ABSTRACT

We analyze a plasmonic gap-mode Fabry-Perot nanocavity containing a metallic nanowire. The proper choice of the cladding layer brings about a decent confinement inside the active region for the fundamental and first-order plasmonic gap modes. We numerically extract the reflectivity of the fundamental and first-order mode and obtain the optical field inside the cavity. We also study the dependence of the reflectivity on the thickness of Ag reflectors and show that a decent reflectivity above 90 % is achievable. For such cavities with a cavity length approaching 1.5 μm, a quality factor near 150 and threshold gain lower than 1500 cm^{-1} are achievable.

Keywords: surface plasmons, semiconductor lasers, nanotechnology

1. INTRODUCTION

There has been significant progress on nanoscale metal-related resonators aiming at an ultrasmall footprint.[1–5] In this paper, we analyze a plasmonic Fabry-Perot (FP) nanolaser based on surface-plasmon-polariton (SPP) gap modes at telecommunication wavelengths around 1.55 μm. The configuration is composed of a truncated waveguide formed by a silver (Ag) nanowire and Ag substrate which sandwich a low-index dielectric gap of silicon dioxide (SiO_2), as indicated in Fig. 1(a). The dielectric gap plays the role of active regions and contains colloidal quantum dots (QDs) as the gain medium.[6,7] The structure is covered by a thick cladding layer, and two Ag-coated end facets function as reflectors, as indicated in Fig. 1(b). The cladding refractive index n_c will be varied in later calculations under a fixed gap height $h = 10$ nm and nanowire radius $r = 70$ nm. The fundamental transverse mode of the guiding structure in Fig. 1, which is usually the focus in typical FP nanocavities, is the most promising for lasing at the ambient environment ($n_c = 1$). On the other hand, we are particularly interested in the case of high-index condition because it corresponds to the deposition of semiconductors as the cladding layer. In such cases, the technologies of microelectronics and silicon photonics, including group-IV and III-V semiconductors, may be further integrated with plasmonics and lead to more functionalities.[8–10] In comparison to the fundamental mode, the first-order mode in the presence of the high-index cladding often exhibits the better field confinement in the active region and higher reflectivity using Ag reflectors. From this point of view, we will look into the lasing characteristics of the first-order mode in high-index cladding materials such as semiconductors.

Further author information:
Shu-Wei Chang: E-mail: swchang@sinica.edu.tw
Tzy-Rong Lin: E-mail: trlin@ntou.edu.tw

Physics and Simulation of Optoelectronic Devices XXII, edited by Bernd Witzigmann, Marek Osinski, Fritz Henneberger, Yasuhiko Arakawa, Proc. of SPIE Vol. 8980, 89801Y · © 2014 SPIE
CCC code: 0277-786X/14/$18 · doi: 10.1117/12.2038718

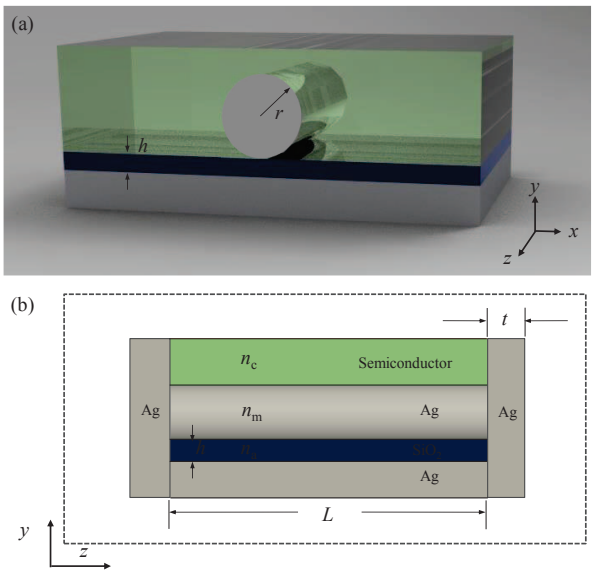

Figure 1. (a) A metallic nanowire is separated from the Ag substrate by the active layer. The structure is embedded in a cladding layer. (b) The side view of the plasmonic gap-mode nanocavity.

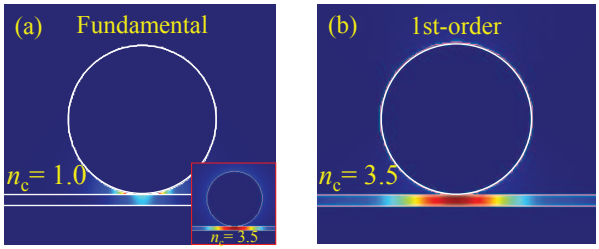

Figure 2. Square magnitudes $|\mathbf{E}(\rho)|^2$ of the cross-sectional profiles for the fundamental mode at (a) $n_c = 1$ (inset: $n_c = 3.5$) and for the first-order mode at (b) $n_c = 3.5$. The height h and radius r are 10 and 70 nm, respectively.

2. DISCUSSION

The SPP gap modes of the structure in Fig. 1 are formed by the coupling between plasmonic modes of the cirular nanowire and surface waves of the gap layer sandwiched by the substrate and cladding. The coupling strengths of the fundamental and first-order SPP gap modes are sensitive to variations of the cladding index n_c. The cross-sectional profile of the FP lasing mode at a low cladding index can be different from that at a high index. We use the two-dimensional (2D) finite-element method (FEM) to compare characteristics of the two modes. In Fig. 2, we show square magnitudes $|\mathbf{E}(\rho)|^2$ of the cross-sectional profiles ($\rho = x\hat{x} + y\hat{y}$ is the transverse coordinate) for the fundamental modes at $n_c = 1$ and first-order modes at $n_c = 3.5$. From Fig. 2(a), the fundamental mode at $n_c = 1$ is localized near the bottom of the nanowire, which is similar to the localized field near tips of metallic bowtie structures.[11] The localized field below the wire bottom does not penetrate into the active region much. However, in the target case of $n_c = 3.5$, the field of first-order mode is tightly confined in the active region below the nanowire and does not spread around lossy regions of the Ag nanowire and substrate. Such an advantage for lasing is, nevertheless, absent for the fundamental mode in the high-index cladding, as can be inferred from the inset of Fig. 2(a). The poorer field confinement in the active region and more significant distribution around the metallic nanowire make the first-order mode less promising for lasing in the presence of semiconductor cladding. Therefore, if we would pick up and design a cross-sectional profile for the lasing mode with semiconductor claddings, the first-order mode should be the choice.

Evolutions of different modes as n_c changes are more easily understood from the waveguide confinement factor Γ_{wg} and modal loss α_i which are relevant to lasing. As shown in Fig. 3(a), Γ_{wg} and α_i of the fundamental and

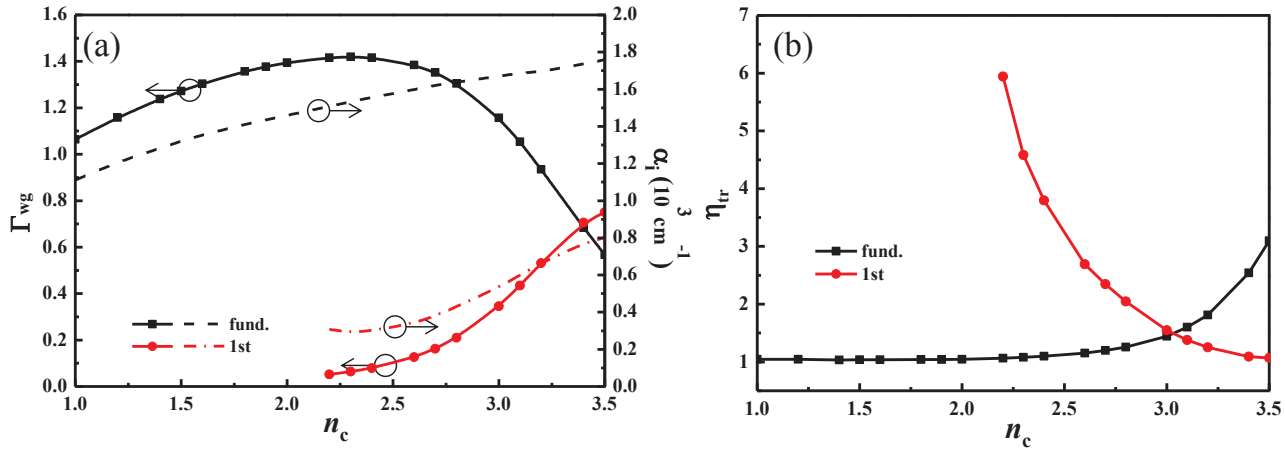

Figure 3. (a) The waveguide confinement factors Γ_{wg} and modal losses α_i, and (b)transparency gains g_{tr} of the fundamental and first-order hybrid gap modes versus n_c at a fixed $h = 10$ nm and $r = 70$ nm. Symbols "fund." and "1st" indicate fundamental and first-order modes, respectively.

first-order modes as a function of the cladding index are calculated. The trends of Γ_{wg} and α_i as n_c varies are different and are directly related to the corresponding mode profiles in Fig. 2. As n_c increases from unity to 3.5, the confinement factor Γ_{wg} of the fundamental mode first increases mildly but then decreases wildly, at which the counterpart of the first-order mode grows sharply. The behavior of Γ_{wg} versus n_c for the fundamental mode just reflects the field evolution in Fig. 2(a), and the enhancement of Γ_{wg} for the first-order mode corresponds to the increasing overlap of the field with the active region. While the variation of α_i with n_c is relatively mild for the fundamental mode, the increase of this parameter for the first-order mode is due to the accompanying penetration into the Ag substrate when the field is more confined in the active region.

From the viewpoint of the lasing threshold, the transparency threshold defined as $g_{tr} = \alpha_i/\Gamma_{wg}$ is the necessary material gain which sustains the propagation of the mode without being attenuated. It is usually desired to minimize g_{tr} under given constraints of guiding structures. In Fig. 3(b), we show the transparency threshold gains g_{tr} of the fundamental and first-order modes corresponding to each pair of curves in Fig. 3(a), respectively. At $n_c = 3.5$ (semiconductors), the transparency threshold of the first-order mode is usually lower than that of the fundamental one. At this stage, to minimize the propagation loss from the metal absorption in the presence of semiconductor claddings, the first-order transverse mode of this plasmonic waveguide should be the target mode.

On the other hand, the mirror loss is another factor hindering the lasing action of the plasmonic nanolaser. As the cavity length L of the FP cavity is shortened, the power leakage from two end facets is enhanced. In fact, with a cavity length L in the (sub)micron range, power leakage from two end facets can easily dominate over the propagation loss, and increasing the reflectivity becomes necessary for the threshold reduction. For this purpose, we consider Ag coatings of a few tens of nanometers at two end facets of the plasmonic cavity as reflectors. Here, we utilize interference patterns between the incident mode and reflected field (standing waves) and the orthogonality theorem of waveguide modes to calculate the modal reflection coefficient and reflectivity of Ag mirrors. In Fig. 4, we show the reflectivities of both the fundamental mode with a low-index surrounding ($n_c = 1$) and the first-order mode in the presence of the semiconductor cladding($n_c = 3.5$). In the latter case, when the thickness t is more than 25 nm, the reflectivity R can be higher than 90 %. Thickening Ag reflectors is indeed an efficient way to enhance the reflectivity and provides a solution to the high threshold. However, for the fundamental mode with the low-index cladding, the reflectivity is restrained and smaller than 80% at the even larger thickness t. If we adopt the cavity resonance of the fundamental guided mode in the presence of the low-index cladding, the Ag coatings do not effectively block the power leakage from edge facets. The corresponding threshold reduction will not be sufficient to make the lasing action potentially sustainable with colloidal QDs. In the following calculations, we will therefore focus on the threshold characteristics of the first-order mode in the target cladding (semiconductor).

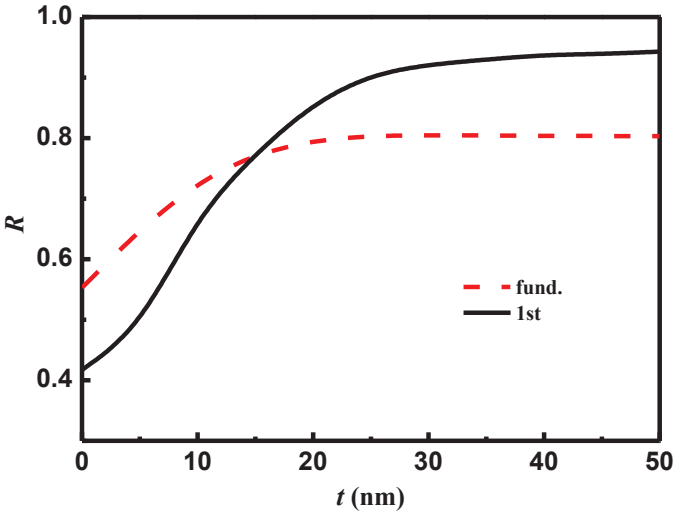

Figure 4. The reflectivities R of the fundamental mode at $n_c = 1$ and first-order mode at $n_c = 3.5$ as a function of the Ag thickness t. The gap height and wire radius are $h = 10$ nm and $r = 70$ nm, respectively.

Table 1. The reflectivities, quality factors, and threshold gains of cavity modes corresponding to mirror thicknesses $t = 0$ (L =1547 nm) and 50 nm (L =1511 nm) at the wavelength of 1.55 μm. The cavity parameters are set as follows: $h = 10$ nm, $r = 70$ nm, and $n_c = 3.5$.

t (nm)	L (nm)	R	Γ_{wg}	g_{th} (cm^{-1})	Q
0	1547	0.506	0.734	7071.4	31.2
50	1511	0.957		1472.5	149.9

We use the FP round-trip oscillation condition to estimate the required cavity length L, quality (Q) factor and threshold gain g_{tr} so that the lasing action at the target wavelength of 1.55 μm is permissible.[12] In Table 1, we list various parameters for two candidate mirror thicknesses $t = 0$ and 50 nm, at cavity lengths L around 1.5 μm which satisfy the FP round-trip phase condition at $r = 70$ nm, $h = 10$ nm, and $n_c = 3.5$. We note that Ag mirrors with a thickness of 50 nm significantly increase the reflectivity (lower the mirror loss) when compared to the case of bare waveguide/air interfaces ($t = 0$).

From Table 1, the quality (Q) factor of the FP cavity mode may exceed 100 (149.9) at $t = 50$ nm and $L = 1511$ nm, and the corresponding threshold gain g_{th} is lowered below 1500 cm^{-1} (1472.5 cm^{-1}). This threshold gain may be sustainable by, for example, colloidal QDs such as PbS with the intense optical pumping.[6,7] To understand the field distribution inside the plasmonic gap cavity, we carry out the 3D FEM simulation for L =1511 nm and t =50 nm at the resonance wavelength of 1.55 μm, which is potentially more promising for lasing than other modes. The transverse profile of the mode on the cross-section (x-y plane) of the cavity is depicted in Fig. 5(a), and the clear standing-wave pattern along the longitudinal direction (z) is shown in Fig. 5(b). In addition to the clear standing-wave pattern along FP cavity (z direction), the mode is also laterally confined (x direction). Due to the high reflectivity of the guided mode at the waveguide/mirror junction, the cross-sectional profile of the 3D mode pattern resembles that of the first-order mode in the infinitely long plasmonic waveguide.

3. CONCLUSION

We have analyzed a plasmonic FP nanocavity with a metallic nanowire embedded in a thick cladding layer. First, two cladding refractive indices of unity (ambience) and 3.5 (semiconductor) are considered. We investigate the effect of dielectric claddings around the nanowire on the fundamental and first-order plasmonic gap modes. Using FEM, we numerically solve guided modes of the plasmonic waveguide at a wavelength of 1.55 μm. The waveguide confinement factors and modal losses of the fundamental and first-order modes are explored as a function of the

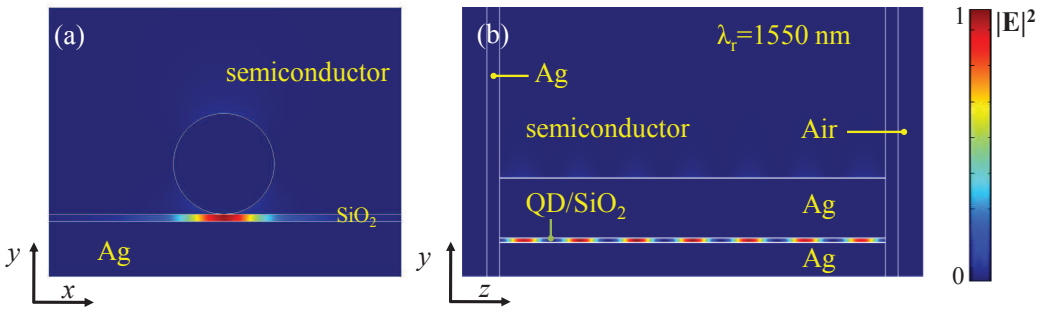

Figure 5. (a) The side view (y-z plane) and (b) front view (x-y plane) of the mode profile corresponding to the case of $L = 1511$ nm in Table 1. The field pattern is excited by a plane wave normally incident onto the Ag mirror from the free space outside the cavity.

cladding index at various gap heights and wire radii. We utilize standing wave patterns from interferences of the incident and reflected fields and the orthogonality theorem of waveguide modes to calculate modal reflection coefficients and reflectivities at cavity ends. The result shows that both the field confinement and reflectivity can be improved with adequate choices of cladding materials. To reduce the mirror loss, we additionally consider silver coatings at two end facets as reflectors. Using silver coatings within a decent thickness range, we show that the reflectivity is substantially enhanced above 90 %. The corresponding cavity performance is evaluated based on the threshold gain and Q factor of FP cavities. At a coating thickness of 50 nm and cavity length of 1.51 μm, the quality factor is about 150, and the threshold gain can be lower than 1500 cm^{-1}.

ACKNOWLEDGMENTS

This work was sponsored by Research Center for Applied Sciences, Academia Sinica, Taiwan, and National Science Council, Taiwan, under Grant numbers NSC-102-2221-E-001-027 and NSC 102-2221-E-019-050. The authors would like to thank Professor Shun Lien Chuang at the Department of Electrical and Computer Engineering, University of Illinois at Urbana-Champaign, for his encouragements and fruitful discussion.

REFERENCES

[1] Schuller, J. A., Barnard, E. S., Cai, W., Jun, Y. C., White, J. S., and Brongersma, M. L., "Plasmonics for extreme light concentration and manipulation," *Nature Mater.* **9**, 193–204 (Mar. 2010).

[2] Hill, M. T., "Status and prospects for metallic and plasmonic nano-lasers [invited]," *J. Opt. Soc. B* **27**, B36–B44 (Nov. 2010).

[3] Ma, R. M., Oulton, R. F., Sorger, V. J., and Zhang, X., "Plasmon lasers: coherent light source at molecular scales," *Laser & Photon. Rev.* **7**, 1–21 (Jan. 2013).

[4] Russell, K. J., Liu, T. L., Cui, S., and Hu, E. L., "Large spontaneous emission enhancement in plasmonic nanocavities," *Nature Photon.* **6**, 459–462 (Jul. 2012).

[5] Russell, K. J. and Hu, E. L., "Gap-mode plasmonic nanocavity," *Appl. Phys. Lett.* **97**, 163115 (Oct. 2010).

[6] Grandidier, J., des Francs, G. C., Massenot, S., Bouhelier, A., Markey, L., Weeber, J.-C., Finot, C., and Dereux, A., "Gain-assisted propagation in a plasmonic waveguide at telecom wavelength," *Nano Lett.* **9**, 2935–2939 (Jul. 2009).

[7] Dai, D., Shi, Y., He, S., Wosinski, L., and Thylen, L., "Gain enhancement in a hybrid plasmonic nano-waveguide with a low-index or high-index gain medium," *Opt. Express* **19**, 12925–12936 (Jul. 2011).

[8] Ozeki, M., "Atomic layer epitaxy of III-V compounds using metalorganic and hydride sources," *Mater. Sci. Rep.* **8**(3), 97–146 (1992).

[9] George, S. M., "Atomic layer deposition: an overview," *Chem. Rev.* **110**(1), 111–131 (2010).

[10] Arnold, D. P., Cros, F., Zana, I., Veazie, D. R., and Allen, M. G., "Electroplated metal microstructures embedded in fusion-bonded silicon: conductors and magnetic materials," *J. Microelectromech. Syst.* **13**, 791–798 (Oct. 2004).

[11] Lin, T. R., Chang, S. W., Chuang, S. L., Zhang, Z., and Schuck, P. J., "Coating effect on optical resonance of plasmonic nanobowtie antenna," *Appl. Phys. Lett.* **97**, 063106 (Aug. 2010).
[12] Cheng, P.-J., Weng, C.-Y., Chang, S.-W., Lin, T.-R., and Tien, C.-H., "Plasmonic gap-mode nanocavities with metallic mirrors in high-index cladding," *Opt. Express* **21**, 13479–13491 (Jun 2013).